treatment of the data provided the rate constants in Table III.

The observed rate constants were partitioned into rate constants for the formation of [3.3.2]propellane (**11**), k_{prop}, and the formation of the remaining aromatic products, k_{arom}. The ratio of these rate constants at each temperature was calculated by least-squares treatment as the slope of the line formed by plotting the concentration of **11** against that of aromatic products, as they varied with flow rates. The calculated, partitioned rate constants are given in Table III.

Gas-Phase Static Kinetics of [3.3.2]Propellane (11). A nearly saturated solution of **11** in *n*-octane as internal standard was prepared. Observed rate constants based on disappearance of starting material relative to internal standard were obtained at 430.2, 450.2, and 469.9 °C. At each temperature, four tubes containing about 10 mg of solution was pyrolyzed for four different lengths of time. Pentane solutions of the products were prepared, and their composition determined by GC analysis (10 ft × $^1/_8$ in. 10% SE-30, oven temperature 80 °C). Four or five injections were made of each time. Plots of natural log of concentration of **11** vs time were linear, and the first-order rate constants were calculated by least-squares treatment of the data.

Gas-Phase Static Kinetics of Bicyclo[3.3.0]oct-1(5)-ene (14). To approximately 60 mg of **14** was added 20 μL of *n*-octane as internal standard. Four samples were pyrolyzed at 450.4 °C for 2, 4, 6, and 8.5 h. Four injections for each tube were made. A plot of natural log of the concentration of **14** vs time was linear and gave a rate constant of 5.13 ± 0.15 × 10^{-5} sec^{-1}.

Determination of Rate Constants for [3.3.2]Propellane (11) Pyrolysis. Rate constants at 450 °C for the formation of **14** and **15** from **11** were estimated by Runge-Kutta integration of the rate equations. The kinetic scheme used for the fit is shown in Scheme III.

Loss of volatile mass was observed in the pyrolyses of **11**, **14**, and, when carried out in sealed tubes, **15**. The observed rate constant for the disappearance of **11** was partitioned into rate constants for product formation and polymerization, k_{prod} and k_{poly}, by a Runge-Kutta calculation. The best fit for the observed product formation, while maintaining $k_{prod} + k_{poly} = k_{obs}$, occurred with $k_{prod} = 1.32 \times 10^{-5}$ and $k_{poly} = 3.81 \times 10^{-5}$. k_2 and k_7 were fixed at these values for the tricyclo[3.3.2.$0^{1,5}$]decane calculation. Considerable loss of volatile mass for **15** was observed in sealed tubes, but due to the speed of this reaction at 450 °C, no attempt was made to quantify it. k_6 was included as a variable in the calculation, while k_4 and k_5 were fixed at the experimentally determined values. Separate static pyrolyses of toluene, ethylbenzene, the xylenes, and indan showed the aromatic products were stable to the reaction conditions.

The concentrations of **11**, **14**, and **15** and aromatic products as a function of time were calculated by integrating the rate equations and varying k_1, k_3, and k_6. Care was taken to match the experimental half-life of **11**, the time and value of the maximum concentration of **14**, and overall volatile mass.

Acknowledgment. This investigation was supported by a grant from the National Science Foundation. The 6-31G* energies were obtained with use of a Cray computer at the Pittsburgh Supercomputing Center with the aid of a grant from that center and also with a TRACE (Multiflow) computer. We thank Dr. M. Frisch and the Multiflow Computer Corp. for their assistance in obtaining some of the energies.

Registry No. 4, 36120-88-4; **4** diradical, 97135-90-5; **7**, 31341-19-2; **7** diradical, 127709-52-8; **8**, 80437-14-5; **9**, 31341-18-1; **9** diradical, 127709-51-7; **10**, 30830-22-9; **10** diradical, 127709-50-6; **11**, 27613-46-3; **11** diradical, 127709-53-9; **12**, 38325-64-3; **12** diradical, 127709-54-0; **13**, 19074-25-0; **13** diradical, 127709-55-1; **14**, 6491-93-6; **15**, 18216-01-8; **16**, 5557-91-5; **17**, 52086-82-5; bicyclo[3.3.0]-7-octen-1-one, 10515-92-1; tricyclo[3.3.2.0]decan-1-one, 5202-23-3.

Integer-Spin EPR Studies of the Fully Reduced Methane Monooxygenase Hydroxylase Component

Michael P. Hendrich,[†] Eckard Münck,*[,†] Brian G. Fox,[‡] and John D. Lipscomb[‡]

Contribution from the Gray Freshwater Biological Institute, The University of Minnesota, Navarre, Minnesota 55392, and Department of Biochemistry, The University of Minnesota, Minneapolis, Minnesota 55455. *Received December 18, 1989*

Abstract: The hydroxylase component of methane monooxygenase contains a binuclear iron cluster in which the iron appears to be oxo or R-oxo bridged. Mössbauer and EPR studies have demonstrated antiferromagnetic coupling for the [Fe(III)Fe(III)] and [Fe(II)Fe(III)] states of the cluster. In the [Fe(II)Fe(II)] form the cluster exhibits an intense X-band EPR signal with zero crossing near $g = 16$, which originates from an electronic system with integer spin. We have studied this signal from 2 to 20 K using a cavity that allows modes where the microwave magnetic field fluctuates either parallel or perpendicular to the static field. We have analyzed the line shapes and the temperature dependence of the spectra with a spin Hamiltonian containing zero-field splitting (D, E) and exchange (J) terms for a pair of $S = 2$ spins. Two coupling schemes, both involving *ferromagnetic* coupling, are compatible with the data. In the scheme for strong coupling ($|J| \gg D$ and $D = 1.2$ cm^{-1}), the $g = 16$ signal results from $\Delta M = \pm 1$ transitions between the two lowest levels of an $S = 4$ multiplet. In the scheme for weak coupling ($J = -0.75$ cm^{-1} and $D_1 = D_2 = -5$ cm^{-1}), the resonance is assigned to $\Delta m_i = 0$ transitions. Simulation of the observed spectra has allowed quantitation of the $g = 16$ signal. This signal represents the majority of the iron in the hydroxylase regardless of the spin-coupling model assumed. Our results demonstrate that integer spin systems with large zero-field splittings are amenable to reliable quantitative analysis.

Soluble methane monooxygenase (EC 1.14.13.25) isolated from *Methylosinus trichosporium* OB3b is a three-component enzyme composed of a reductase (40 kDa, containing one FAD and one [2Fe 2S] cluster), component B (16 kDa, no cofactors or metal ions), and hydroxylase (245 kDa, containing four non-heme iron atoms).[1] The function of the enzyme system in vivo is to catalyze the O_2- and NADH-dependent oxidation of methane to methanol.[2] This is the first step in the catalytic pathway utilized by methanotrophic bacteria to provide carbon and energy for growth. The enzyme system adventitiously catalyzes the oxidation of many other saturated, unsaturated, and cyclic hydrocarbons, some at rates comparable to that of methane turnover.[3] While all three protein components are required for NADH-dependent substrate oxidation, we have recently shown that the hydroxylase alone will

* Author to whom correspondence should be addressed.
† Gray Freshwater Biological Institute.
‡ Department of Biochemistry.

(1) Fox, B. G.; Froland, W. A.; Dege, J.; Lipscomb, J. D. *J. Biol. Chem.* **1989**, *264*, 10023-10033.
(2) Dalton, H. *Adv. Appl. Microbiol.* **1980**, *26*, 71-87.
(3) (a) Higgins, I. J.; Best, D. J.; Hammond, R. C. *Nature* **1980**, *256*, 561-564. (b) Green, J.; Dalton, H. *J. Biol. Chem.* **1989**, *264*, 17698-17703.

0002-7863/90/1512-5861$02.50/0

support turnover upon reduction by dye-mediated chemical reductants.[1]

The structure of the iron centers of the hydroxylase isolated from several different bacterial sources has been investigated with various spectrscopic techniques. It has been shown that the catalytic center can be stabilized in three redox states. Mössbauer studies[4] have shown that the oxidized protein contains a cluster consisting of an even number (most probably two) of high-spin Fe^{3+} ions, which are antiferromagnetically coupled to yield a diamagnetic ground state. In the mixed-valent state (i.e. one-electron reduced) an EPR signal is observed[1,4,5] reminiscent of those elaborated by enzymes and proteins containing antiferromagnetically coupled oxo-bridged binuclear [Fe(II)Fe(III)] clusters.[6] EXAFS measurements[7] of the mixed-valent hydroxylase are consistent with this assignment and further suggest that the bridging oxygen is protonated or otherwise triply liganded. Quantitation of the Mössbauer and EPR spectra obtained from the *M. trichosporium* OB3b hydroxylase has shown that the highest activity preparations contain approximately two oxo-bridged binuclear clusters per molecule.[1] The occurrence of a cluster of this type in an oxygenase is unprecedented. Since Mössbauer spectra show that all of the iron occurs as part of an oxo-bridged binuclear cluster, and since no other metals, cofactors, or organic radicals are present in higher than trace levels, it must be assumed that the iron cluster is responsible for catalysis.

The fully reduced state of the cluster [Fe(II)Fe(II)] is of particular interest because the results of chemically driven turnover experiments strongly suggest that this is the only state capable of supporting turnover.[1] During our studies of the fully reduced hydroxylase, we observed a low-field EPR signal at $g = 16$.[1,4] Mössbauer studies show only high-spin ($S = 2$) Fe^{2+} when this EPR signal has maximal intensity, suggesting that the observed resonance represents a system with integer electronic spin. Such low-field EPR signals have also been observed for integer-spin states of other proteins containing spin-coupled metals centers such as ferredoxin II from *Desulfovibrio gigas*,[8] the azide complex of deoxyhemerythrin,[9,10] and cytochrome oxidase[10,11] and from a variety of integer-spin model complexes.[12] Because methods for analyzing and quantitating such integer-spin signals have only recently emerged,[10,13] the relevance of the observed signals has not been adequately assessed for the hydroxylase or any other protein or model complex. Moreover, only one attempt has been made to describe the observed EPR signal of a binuclear iron–oxo protein with a spin-coupling model;[9] this report did not provide analysis of the line shape of the spectra and the mechanism proposed for the transition probability underestimated the observed intensity by many orders of magnitude.

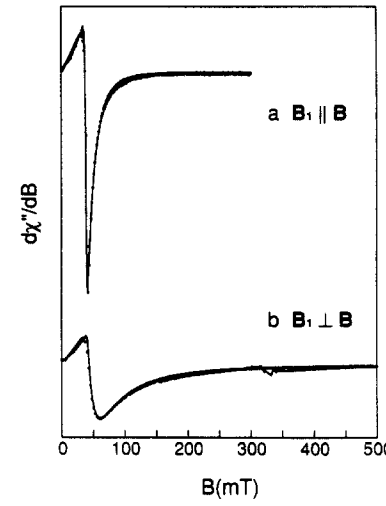

Figure 1. EPR spectra (—) and simulations (···) of the fully reduced methane monooxygenase hydroxylase component at 4 K using microwave field B_1 parallel (a) and perpendicular (b) to the static field **B**. Simulation parameters: $D = 1.2$ cm^{-1}; $E/D = 0.16$; $\sigma_{E/D} \approx 0.07$ (1 standard deviation); $g_y = 2.00$ for the ground doublet of an $S = 4$ multiplet. Instrumental parameters: microwave frequency, 9.1 GHz at 2 mW (unsaturated); modulation, 100 kHz at 0.8 mT(pp) gain, 1.25×10^5; dB/dt, scan rate, 1 mT/s; filter, 0.5 s. Protein data: protein concentration, 1 mM after addition of reductants and mediators; specfic activity, 500; 2.3 mol of Fe/mol of protein (~0.9 mM oxidized iron clusters). Mössbauer studies of this sample have been previously reported.

Here we describe further EPR studies of the $g = 16$ signal observed from the methane monooxygenase hydroxylase. Improved methods for quantitative simulation are employed that indicate that the signal represents the majority of the iron in the fully reduced hydroxylase. The simulations show that iron is contained in a cluster consisting of two high-spin ($S = 2$) ferrous ions that are ferromagnetically coupled. Two spin-coupling models are developed that account for the observed data.

Materials and Methods

The purification and characterization of the hydroxylase component of the soluble methane monooxygenase from *M. trichosporium* OB3b was as previously reported.[1,5a] The hydroxylase sample used for these studies was an aliquot of the Mössbauer sample of ref 4. The hydroxylase was converted to the fully reduced state by using sodium dithionite as a reductant in the presence of the redox mediators methyl viologen and proflavin.[1,4] The total cluster concentration of the sample was determined by measuring the total iron concentration by plasma emission spectroscopy (Soil Sciences, University of Minnesota, St. Paul). The determination was corrected for a small amount of adventitious iron by using the Mössbauer spectrum of the oxidized sample.

X-band EPR spectra were recorded with a Bruker ER 200D spectrometer using an Oxford liquid helium flow cryostat and a Varian Model E-236 bimodal cavity.[10,13] Computer simulations were generated by using either perturbation expressions for the zero-field splitting and transition probability or by diagonalization of the spin Hamiltonian of eq 3. The simulation program is formulated in accordance with eq 12 of ref 10 with modifications appropriate for an $S = 4$ spin Hamiltonian. A version of this program for an $S = 2$ Hamiltonian was previously shown to give quantitative agreement between Kramers and non-Kramers signal intensitites. For the quantitative analyses, the program diagonalizes eq 3 at each point in a grid formed by variation of an angle and a zero-field splitting (ZFS) parameter. Typical calculations require approximately 1 min of processor time on a CDC Cyber 175 computer. A detailed account of the computational procedures will be published elsewhere.

Crystals of Fe^{2+} doped into zinc fluosilicate were used as the quantitation standard.[10] The percentage of iron to zinc determined by plasma emission spectroscopy was 1.49 ± 0.03%.

For studies of the temperature dependence of the $g = 16$ signal, a 1 mm o.d. capillary tube containing Fe^{3+}EDTA ($D = 0.7$ cm^{-1}, $E/D = 0.3$ cm^{-1})[14] was imbedded into the frozen hydroxylase sample for use as a temperature calibration standard. The signal intensity for Fe^{3+}EDTA as a function of temperature is rather flat near 3 K. This results in the

(4) Fox, B. G.; Surerus, K. K.; Münck, E.; Lipscomb, J. D. *J. Biol. Chem.* **1988**, *263*, 10553–10556.
(5) (a) Fox, B. G.; Lipscomb, J. D. *Biochem. Biophys. Res. Commun.* **1988**, *154*, 165–170. (b) Woodland, M. P.; Patil, D. S.; Cammack, R.; Dalton, H. *Biochim. Biophys. Acta* **1986**, *873*, 237–242.
(6) Que, L., Jr.; Scarrow, R. C. In *Metal Clusters in Proteins*; Que, L., Jr., Ed.; ACS Symposium Series 372; Americal Chemical Society: Washington, DC, 1988; Chapter 8, and the references cited therein.
(7) Prince, R. C.; George, G. N.; Savas, J. C.; Cramer, S. P.; Patel, R. N. *Biochim. Biophys. Acta* **1988**, *952*, 220–229. (b) Ericson, A.; Hedman, B.; Hodgson, K. O.; Green, J.; Dalton, H.; Bentsen, J. G.; Beer, R. H.; Lippard, S. J. *J. Am. Chem. Soc.* **1988**, *110*, 2330–2332.
(8) Papaefthymiou, V.; Girerd, J.-J.; Moura, I.; Moura, J. J. G.; Münck, E. *J. Am. Chem. Soc.* **1987**, *109*, 4703–4710.
(9) (a) Reem, R. C.; Solomon, E. I. *J. Am. Chem. Soc.* **1987**, *109*. 1216–1226. (b) Reem, R. C.; Solomon, E. I. *J. Am. Chem. Soc.* **1986**, *108*, 8323–8325.
(10) Hendrich, M. P.; Debrunner, P. G. *Biophys. J.* **1989**, *56*, 489–506.
(11) (a) Brudvig, G. W.; Morse, R. H.; Chan, S. I. *J. Magn. Reson.* **1986**, *67*, 189–201. (b) Dunham, W. R.; Sands, R. H.; Shaw, R. W.; Beinert, H. *Biochim. Biophys. Acta* **1983**, *748*, 73–85. (c) Hagen, W. R. *Biochim. Biophys. Acta* **1982**, *708*, 82–98.
(12) (a) Borovik, A. S.; Que, L., Jr. *J. Am. Chem. Soc.* **1988**, *110*, 2345–2347. (b) Drexheimer, S. L.; Gohdes, J. W.; Chan, M. K.; Hagen, K. S.; Armstrong, W. H.; Klein, M. P. *J. Am. Chem. Soc.* **1989**, *111*, 8923–8925. (c) Tolman, W. B.; Bino, A.; Lippard, S. J. *J. Am. Chem. Soc.* **1989**, *111*, 8522–8523.
(13) Hendrich, M. P.; Debrunner, P. G. *J. Magn. Reson.* **1988**, *78*, 133–141.
(14) (a) Aasa, R. *J. Chem. Phys.* **1970**, *52*, 3919–3930. (b) Lang, G.; Aasa, R.; Garbett, K.; Williams, R. J. P. *J. Chem. Phys.* **1971**, *55*, 4539–4548.

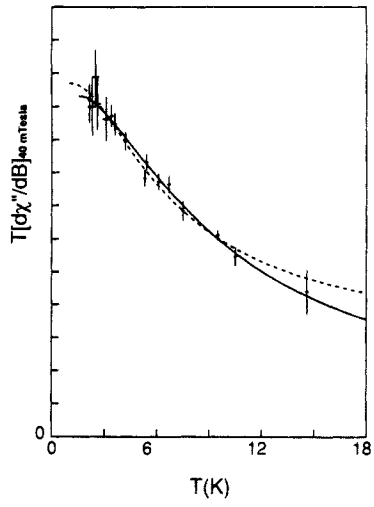

Figure 2. Temperature dependence of the hydroxylase signal of Figure 1a. Signal intensity is determined as the depth of the valley at $B = 40$ mT. The theoretical lines were calculated by diagonalizations of either eq 1 for $J = -0.7$ cm^{-1}, $D_i = -5$ cm^{-1}, and $E_i/D_i = 0.27$ (—); or eq 3 for $D = +1.2$ cm^{-1} and $E/D = 0.2$ (- - -).

relatively large temperature uncertainties evident in Figure 2 for the data obtained near 3 K.

Results and Discussion

Figure 1 shows X-band EPR spectra of the fully reduced hydroxylase from *M. trichosporium* OB3b. The spectra were recorded at $T = 4$ K under conditions where the magnetic microwave field $\mathbf{B}_1$ is either parallel or perpendicular to the static field $\mathbf{B}$. The data were recorded with nonsaturating microwave power, i.e., the signal is proportional to $\mathbf{B}_1$ at all points in the spectrum. The position of the resonance (zero crossing near $g = 16$ at X band) and the observation of enhanced intensity in parallel mode (Figure 1a) are characteristic of systems with integer electronic spin.[10,13] Assignment of the observed signal to an integer-spin system is supported by two experimental observations: (1) any signal from a typical half-integer-spin system would be suppressed by at least 2 orders of magnitude in parallel mode; (2) a Mössbauer study of this particular sample (Figure 1C and D of ref 4) showed that all iron was high-spin ferrous. In contrast to the resonance condition for Kramers systems, $h\nu = g\beta B$, signals from integer-spin systems as observed here typically originate from quasi-degenerate doublets for which the resonance condition can be written as

$$(h\nu)^2 = \Delta^2 + (\tilde{g}\beta_e B)^2 \quad (1)$$

In eq 1, Δ is the splitting of the two levels in zero applied field, $\tilde{g} = g_{\text{eff}} \cos \alpha$, where α is the angle between the static field $\mathbf{B}$ and an appropriate molecular axis, and g_{eff} is the effective g value of the doublet at $\alpha = 0$. Note that the resonance condition is quadratic in B when $\beta_e B$ is comparable to Δ. For the strong coupling scheme discussed below, the "appropriate" molecular axis is the y axis of the zero-field splitting tensor of eq 2.

Figure 2 shows the temperature dependence of the $g = 16$ signal of Figure 1a, plotted as signal amplitude times T versus T. The data, recorded to $T = 2$ K, show that the EPR-active doublet is the ground state. Consideration of the temperature dependence with various level schemes shows that the next excited set of levels is at an energy of approximately 4–8 cm^{-1}. One further observation is pertinent for the following discussion. Extensive attempts to simulate the hydroxylase spectra of Figure 1 with the assumption that the signal originates from uncoupled $S = 2$ sites failed on two grounds: (1) the line shapes of the signals could not be matched; and (2) the intensity of the hydroxylase signal is 2 orders of magnitude larger than those we have observed for mononuclear $S = 2$ complexes.[10,13] This indicates that the EPR signal originates from an exchange-coupled system.

The energy levels of two exchange-coupled high-spin ($S_1 = S_2 = 2$) ferrous sites can be described in the framework of a spin Hamiltonian by

$$\hat{H} = J\mathbf{S}_1\cdot\mathbf{S}_2 + \sum_{i=1}^{2} [(D_i(S_{z_i}^2 - 2) + E_i(S_{x_i}^2 - S_{y_i}^2) + \beta_e \mathbf{S}_i\cdot\mathbf{g}_i\cdot\mathbf{B}] \quad (2)$$

where J is the exchange coupling constant, D_i and E_i are the axial and rhombic zero-field splitting (ZFS) parameters, and $\mathbf{g}_i$ are the g tensors of the uncoupled sites ($i = 1, 2$). We will assume that all tensors in eq 2 have a common principal axis system, more out of necessity to keep the number of unknowns manageable than from experimental evidence[15] (but see below). It will be useful to discuss eq 2 for two limiting cases, namely for strong, $|J| \gg |D_i|$, and weak, $|J| \ll |D_i|$, coupling.

For *strong* exchange coupling, the system consists of multiplets of total spin S. The splittings of each multiplet can be described by a spin Hamiltonian

$$\hat{H} = D[(S_z^2 - \tfrac{1}{3}S(S+1)] + E(S_x^2 - S_y^2) + \beta_e\cdot\mathbf{S}\cdot\mathbf{g}\cdot\mathbf{B} \quad (3)$$

where D, E, and $\mathbf{g}$ can be computed for each multiplet from the corresponding quantitites of eq 2 by application of the Wigner–Eckart theorem; a variety of useful expressions have been given by Scaringe et al.[16] Since the electronic ground state of the reduced hydroxylase is a quasi-degenerate doublet, the coupling must be ferromagnetic; antiferromagnetic coupling would result in a diamagnetic ($S = 0$) ground state. For an $S = 4$ multiplet a suitable quasi-degenerate doublet can result for positive and negative D values. For $D < 0$ and $E \neq 0$, the ground doublet is essentially composed of the $|4^{\pm}\rangle = (|4,+4\rangle \pm |4,-4\rangle)/2^{1/2}$ levels where $|SM\rangle = |4,M\rangle$ refers to the coupled representation. Reem and Solomon[9] have assigned the EPR signal of azidodeoxyhemerythrin to transitions between the $|4^{\pm}\rangle$ levels. However, this type of transition does not describe the $g = 16$ resonance of the reduced hydroxylase, for the following reason. The splitting of the $|4^{\pm}\rangle$ states is in a good perturbative approximation given by $\Delta = (35/16)D(E/D)^4$. Since E/D can be confined to the range $0 \leq E/D \leq {}^1/_3$, the minimum D value for a fixed Δ is obtained for $E/D = {}^1/_3$. The simulations of Figure 1 require $\Delta \approx 0.2$ cm^{-1} (see below). From this Δ value, the calculated $-D \geq 7$ cm^{-1} would place the first set of excited levels at an energy greater than $6.2|D| \approx 43$ cm^{-1}. This is in conflict with the observed temperature dependence of the $g = 16$ resonance, which requires that the first set of excited states be in the range 4–8 cm^{-1}. The observed EPR signal, however, can be fitted to an $S = 4$ multiplet if one assigns the transition to a different pair of levels.

Figure 3 shows the energy levels of an $S = 4$ multiplet for $D > 0$ as a function of E/D. It can be seen that the splitting Δ between the two lowest levels decreases with increasing E/D. The expression given above shows that the two levels are separated by $\Delta = 0.028D$ in the rhombic limit. Thus, for D values up to 11 cm^{-1} one can obtain an E/D value for which Δ is smaller than the X-band microwave quantum ($h\nu \approx 0.3$ cm^{-1}). For $E/D < 0.2$ and $B = 0$, the two levels are predominantly $|0\rangle = |4,0\rangle$ and $|1^-\rangle = (|4,+1\rangle - |4,-1\rangle)/2^{1/2}$. For these levels, one can observe an allowed $\Delta M = \pm 1$ transition with substantial transition probability, $|\langle 0|S_y|1^-\rangle|^2 = S(S+1)/2 = 10$.

For $D > 0$ and $E/D = 0.16$, the data of Figures 1 and 2 can be fit to an $S = 4$ multiplet. From a least-squares fit of the temperature dependence of the $g = 16$ signal to the energy level spacings, we obtained $D = 1.2$ cm^{-1} (dashed line in Figure 2). This set of ZFS parameters, together with $g_x = g_y = g_z = 2.00$ produce the desired Δ value and correct Zeeman splittings for the quasi-degenerate doublet. As described previously,[10,13] the line shapes of integer-spin signals are dominated by strain of the ZFS parameters. The line shapes of the spectra of Figure 1 could be modeled by assuming that the rhombic ZFS parameter E/D has a Gaussian distribution width $\sigma_{E/D} = 0.07$. Since $(d\Delta/dE)/(d\Delta/dD) \approx 11$ at $E/D = 0.16$, a distribution in D has a negligible effect on the spectrum and thus need not be considered for the

(15) Reem and Solomon[9a] have published, for $B = 0$, plots of the system energies versus D_i/J using the same simplifying assumptions.

(16) Scaringe, R. P.; Hodgson, D. J.; Hatfield, W. E. *Mol. Phys.* **1978**, *35*, 701–713.

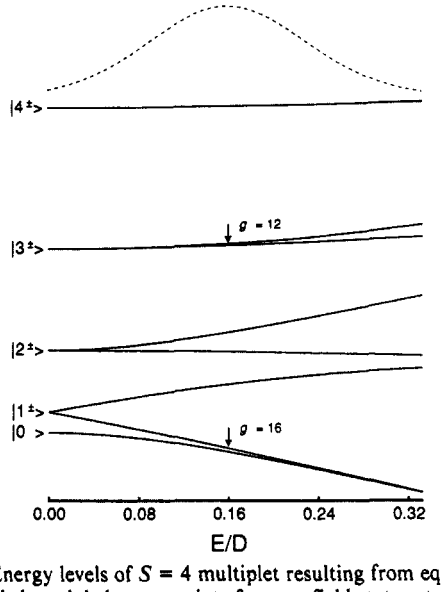

Figure 3. Energy levels of $S = 4$ multiplet resulting from eq 3 for $B = 0$. The levels have labels appropriate for zero-field states at small E/D values; $|M^{\pm}\rangle = (|4,M\rangle \pm |4,-M\rangle)/2^{1/2}$. The lower arrow points at the two levels associated with the X-band resonance at $g = 16$. The upper arrow refers to a possible excited-state resonance at $g = 12$. The splitting of the $|4^{\pm}\rangle$ levels is too small to be resolved in this graph. The Gaussian curve (dotted line) centered at $E/D = 0.16$ with $\sigma_{E/D} = 0.07$ illustrates the distribution of E/D values.

simulations. We wish to stress that the intensity and line shape of the perpendicular mode spectrum of Figure 1b is correctly determined from a fit to the parallel mode spectrum of Figure 1a without use of any adjustable parameters. From extensive spectral simulations with various combinations of E/D, $\sigma_{E/D}$, and g_y, combined with fits to the data of Figure 2, the following uncertainties are estimated: $D = 1.2 \pm 0.2$ cm^{-1}; $E/D = 0.16 \pm 0.03$; $\sigma_{E/D} = 0.07 \pm 0.02$; $g_y = 2.00 \pm 0.05$.[17]

Inspection of the level scheme of Figure 3 suggests that one might also observe EPR transitions between the $|3^{\pm}\rangle$ or $|4^{\pm}\rangle$ levels for the case in which $E/D = 0.16$. However, the transition probability between the $|4^{\pm}\rangle$ levels is vanishingly small. For the $|3^{\pm}\rangle$ levels, a resonance would be observed at $g = 12$ with a transition probability roughly 20% of that calculated for the ground doublet. The reduced transition probability coupled with substantially smaller population factor (0.15 at 15 K) would make observation of this resonance quite difficult. Spectra obtained at 15 K and 23 K indicate a weak shoulder at $g = 12$. Assignment of this shoulder to an excited-state resonance is quite tentative, however, since increased relaxation rates lead to spectral broadening at these temperatures.

The quoted values for D and E/D yield a splitting $\Delta^{\circ} = 0.2$ cm^{-1}, where Δ° is determined from the central value of E/D for the ground doublet. This doublet has an easy direction of magnetization along the y axis; from eq 3 we compute $g_{eff} = 15.3$ along the y axis, while $g_{eff} = 1.0$ and 0.0 along the x and z axes, respectively. Owing to the uniaxial nature of the doublet, the EPR spectra are sensitive essentially to only g_y. We have stated that the observed signals can also be described by eq 1. The use of eq 1 in the final analysis is somewhat limited, however, because a Gaussian distribution in E/D gives rise to a skewed symmetric distribution in Δ. Nevertheless, eq 1 is useful as a starting point for an analysis because it allows one to obtain values for Δ and

(17) We would like to comment on a subtle point that has not yet been resolved. The line shapes of Figure 1a and b are best reproduced by using a distribution in E/D centered at $E/D = 0.16$. A fit of the temperature dependence of the $g = 16$ signal to the energy levels for $E/D = 0.16$ gives $D = 1.4$ cm^{-1}. However, by using the valley at 40 mT as a measure of signal amplitude for the data of Figure 2, we favor molecules of the population that have a slightly larger than average E/D. Thus, the best fit to the temperature dependence was obtained for $D = 1.2$ cm^{-1} and $E/D = 0.20$. The spectral simulations of Figure 1a and b treat the distributions properly and should, therefore, give a better measure of E/D.

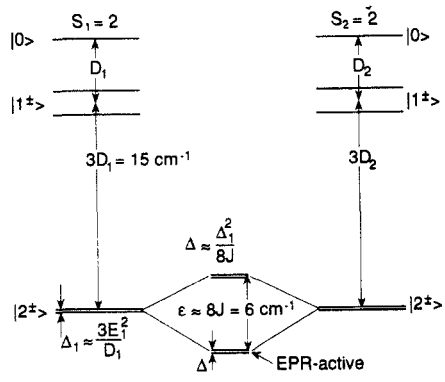

Figure 4. Energy levels in the weak coupling scheme. It is assumed that the zero-field splitting tensors of the two ferrous sites are equal and collinear. The diagram is drawn for $D_1 = D_2 < 0$, $J < 0$ (ferromagnetic coupling), and $J \ll D_i$. The exchange splitting is only indicated for the $|2^{\pm}\rangle$ states; for clarity the exchange interactions between the $|0\rangle$ and $|1^{\pm}\rangle$ states are not considered in the figure. The assumption of equal ZFS tensors is convenient but not crucial for the interpretation of the $g = 16$ resonance.

g_{eff}, which can be used to identify suitable regions in the parameter spaces of eqs 2 and 3.

The preceding discussion has assumed that $|J| \gg |D_i|$. Since the zero-field splitting terms of eq 2 mix multiplets, with mixing proportional to D_i/J, the assumption $|J| \gg |D_i|$ assures a pure $S = 4$ ground multiplet. Actually, the EPR properties of the $S = 4$ multiplet are essentially unchanged even when $|J|$ is only moderately larger than $|D_i|$. Thus, the preceding analysis holds for $|J| \gtrsim 1.5|D_i| \approx 3.45D$ where we have used the relation $D_i = 2.3D$.[16] Thus, in the *strong* coupling scheme we obtain $-J \gtrsim 4$ cm^{-1}.

Figure 4 shows an energy level diagram for the *weak* coupling scheme. In this scheme, the EPR data of the reduced hydroxylase can be interpreted by assuming negative values for D_1 and D_2 and by keeping $|J| \gtrsim {}^1/_3|D_i|$. In the weak coupling scheme, the $|2^{\pm}\rangle = (|2,+2\rangle \pm |2,-2\rangle)/2^{1/2}$ states of both ferrous ions combine to form a quartet, which is split by the exchange interaction, $JS_{1z}S_{2z}$, into two quasi-degenerate doublets. The order of the doublets depends on the sign of J. For ferromagnetic coupling the lower doublet is EPR-active with a selection rule $\Delta m_i = 0$, whereas the excited-state doublet has vanishing EPR intensity.[18] The population decrease of the ground doublet at low temperatures reflects mainly the population of the EPR-silent doublet at energy $\epsilon \approx 8J$; this affords a direct measure of J. A fit to the data of Figure 2 (solid line) yielded $J = -0.75 \pm 0.25$ cm^{-1} and $D_1 = D_2 = -5 \pm 1$ cm^{-1}. The splitting of the quasi-degenerate ground doublet is given by $\Delta \approx \Delta_1^2/8J$, where $\Delta_1 \approx 3E_1^2/D_1$ is the splitting of the $|2^{\pm}\rangle$ doublet of the ferrous ions in zero field. The value $E_1/D_1 = 0.27$ produces the required $\Delta^{\circ} = 0.2$ cm^{-1}, a $g_{eff} = 15.4$, and a transition probability that is within 2% of that of the strong coupling scheme. The value $\sigma_{E_1/D_1} = 0.05$ yields a skewed symmetric distribution of Δ similar to that obtained in the strong coupling scheme. Since these four parameters essentially define the EPR spectrum, simulations generated with this parameter set will produce spectra similar to those obtained for the strong coupling case. The results are not significantly affected if $D_1 \neq D_2$ provided that the D_i values are large enough to separate the $|0\rangle$ and $|1^{\pm}\rangle$ levels from the $|2^{\pm}\rangle$ states. The splitting of the ground doublet is then $\Delta \approx \Delta_1\Delta_2/8J$.

The effects of removing the constraint of coaxial D tensors are not fully understood. Since the $|2^{\pm}\rangle$ doublets of the weak coupling scheme are uniaxial along the z axes of the ZFS tensors of the individual ions, the EPR resonance depends most sensitively on the angle β between these axes. We have studied the effects of the variation of β and have obtained satisfactory matches to the data for $0 < \beta < 30°$. In the strong coupling scheme, information

(18) m_i refers to the magnetic quantum number m_1, m_2 of the $|S_1, m_1\rangle|S_2, m_2\rangle$ representation.

about the individual ZFS tensors and their spatial relation is lost.

The preceding analysis suggests that the $g = 16$ resonance represents a spin-coupled pair of Fe^{2+}. The most compelling argument for spin coupling is the observation that the intensity of the observed signal is about 100 times larger than those typically observed for isolated Fe^{2+} sites. The coupled system exhibits enhanced intensity because of two multiplicative effects: (1) the larger moment of the electronic state of the coupled system increases the transition probability by approximately 2.5–4-fold relative to the $S = 2$ state of an uncoupled Fe^{2+}. (2) We will describe elsewhere that a given distribution of E_1/D_1 values will yield a distribution of Δ values that is narrower for the coupled $S = 4$ than for the uncoupled $S = 2$ state, resulting in a pronounced increase in signal amplitude.[19] With the knowledge that the $g = 16$ resonance represents a coupled system, the spin concentration can be determined by comparing the simulated spectrum to that of a standard. It was shown previously[10] that Fe^{2+} doped into zinc fluosilicate is a suitable standard. An intensity normalization factor was determined by comparison with this standard and used according to method 1 of ref 10 to give an $S = 4$ spin concentration of 0.7 ± 0.1 mM for the hydroxylase sample studied here. The total cluster concentration of the sample *prior to reduction* was estimated to be ~0.9 mM from the total iron concentration corrected for adventitious iron by using the Mössbauer spectrum of the sample (see Materials and Methods). The Mössbauer spectrum of the *reduced* sample is consistent with the majority of the Fe^{2+} residing in spin-coupled clusters.[20] However, comparison of the spectrum of this sample with those of other preparations suggests that as much as 20% of the Fe^{2+} may reside in other environments that may not yield the $g = 16$ signal. Thus, between 70% and 90% of the iron in the sample is accounted for by the $g = 16$ EPR resonance, clearly indicating that the signal represents a biologically and spectroscopically relevant species.

The only other known protein containing a coupled binuclear iron cluster with a ferromagnetic ground state, azidodeoxyhemerythrin,[9,10] exhibits an integer-spin EPR signal similar to that of the reduced hydroxylase. Reem and Solomon[9] have assigned the signal to $\Delta M = \pm 1$ transitions between the $|4^{\pm}\rangle$ levels of an $S = 4$ system. In order to make $\Delta M = \pm 1$ transitions feasible, these authors have invoked level mixing by the Zeeman term. However, one can readily calculate that the proposed transitions would be extremely weak and would give rise to signal intensities many orders of magnitude less than observed. It is possible that the azidodexoyhemerythin resonance reflects a $\Delta M = 0$ transition between the $|4^{\pm}\rangle$ levels although an appropriate Δ value would, as discussed above, require unreasonably large D values. Perhaps, interpretations as proposed here may also be applicable for azidodeoxyhemerythin.

The conclusions reached here are solely based on EPR spectroscopy. In order to obtain more information on this system, other techniques such as magnetometry, Mössbauer spectroscopy, and magnetic circular dichroism spectroscopy must be applied. Interpretation of the data from these techniques is expected to be complex. For example, analysis of the Mössbauer spectra is hampered by the task of determining an almost unmanageable number of unknowns; if the two iron sites are inequivalent and the symmetry is low, as a many as 20 unknown hyperfine parameters are added to the already formidable number of unknowns of eq 2. The current analysis of the results, made possible by the adoption of limiting assumptions, is offered as a reasonable and useful approximation pending more detailed studies.

The studies reported here demonstrate that estimates of the parameters D, J, E/D, and $\sigma_{E/D}$ can be obtained directly from analysis of the integer-spin EPR spectra. The spectral simulation techniques utilized here allow, for the first time, quantitation of the integer-spin EPR signal of a metalloprotein. Moreover, our studies show that the $g = 16$ resonance represents the majority of the iron in the diferrous hydroxylase and not a minority species. Through the use of integer-spin EPR studies, the involvement of this pivotal oxidation state in the catalytic cycle of the methane monooxygenase reaction can now be explored quantitatively.

Acknowledgment. This work was supported by NIH Grants GM40466 (J.D.L.), GM22701 (E.M.), a grant from the NSF-sponsored Center for Biological Process Technology of the University of Minnesota (J.D.L.) and a contract from Amoco Corp. (J.D.L). M.P.H. acknowledges an NIH Postdoctoral Fellowship (GM12996). B.G.F. acknowledges a USPHS Training Grant and a Doctoral Dissertation Fellowship from the Graduate School of the University of Minnesota. We also thank Dr. Peter Debrunner for the use of the EPR spectrometer with which the temperature-calibrated experiments were performed.

(19) For example, for the $|4^{\pm}\rangle$ doublet of the $S = 4$ multiplet, we have $\Delta_4 = (^{35}/_{16})(E_1/D_1)^4(D_1/2.3)$; for the $|2^{\pm}\rangle$ doublet of an $S = 2$ system, the corresponding splitting is $\Delta_2 = 3(E_1/D_1)^2$. Assuming that only E_1 is distributed, we obtain $d\Delta_4 = 0.64(E_1/D_1)^2\, d\Delta_2$. A further narrowing by about a factor 2 is obtained when the variations in Δ_4 and Δ_2 are expressed in B space. For $E_1/D_1 = {}^1/_3$, the narrowing is about 30-fold.

(20) Mössbauer spectra recorded at 1.5 K of the reduced sample studied here show that the majority of the Fe^{2+} exhibits sizeable magnetic hyperfine interactions already in a moderate (~0.2 T) applied magnetic field. This response is typical for an integer-spin system with a quasi-degenerate ground state,[9] in fundamental agreement with our EPR results.